supplementary material for "Degradation Accordant Plug-and-Play for Low-Rank Tensor Completion"

Anonymous IJCAI Submission
Paper ID 1331

Abstract

In this Supplementary Material, we provide i) the update of multipliers, ii) experimental results on the MRI data, iii) additional results on color images, videos, and multispectral images (MSIs).

1 Multipliers updating

At the k-th iteration, multipliers in our method are updated as follows

$$\begin{cases} \Lambda_1^{k+1} = \Lambda_1^k + \beta_1(\mathcal{A}(\mathcal{X}^{k+1}) - b) \\ \Lambda_2^{k+1} = \Lambda_2^k + \beta_2(\mathcal{A}(\mathcal{X}^{k+1}) - \mathcal{A}(\mathcal{Y}^{k+1})) \\ \Lambda_3^{k+1} = \Lambda_3^k + \beta_3(\mathcal{Y} - \mathcal{Z}^{k+1}) \end{cases} \tag{1}$$

2 Experimental Settings

For the readers' convenience, we restate our settings for experiments here. Compared methods are: the Tucker-rank based method HaLRTC[1] [Liu *et al.*, 2013], a t-SVD based method (TNN)[2] [Zhang and Aeron, 2017], a DCT induced TNN minimization method (DCTNN)[3] [Lu *et al.*, 2019], a framelet represented TNN minimization method (FTNN)[4] [Jiang *et al.*, 2020], a deep denoiser regularized TNN minimization method (DP3LRTC)[5] [Zhao *et al.*, 2020], and a deep video inpainter called Onion-peel networks (OPN)[6] [Oh *et al.*, 2019].

For all experiments, two numerical metrics are employed, including the Peak signal-to-noise ratio (PSNR), the structural similarity index (SSIM) [Wang *et al.*, 2004]. Higher PSNR and SSIM values mean better performance. Additionally, we introduce the mean spectral angle mapper (SAM) for MSIs, and lower SAM indicates better results. We report results on color images, videos, and multispectral images in the following part. Please refer to Supplementary Material for results on the MRI data and the parameter analysis.

The training images of the CRUnet consists of 400 images from the Berkeley segmentation dataset (BSD) [Chen and Pock, 2016], 900 images of the DIV2K dataset [Timofte *et al.*, 2017], 4744 images from the Waterloo Exploration Database [Ma *et al.*, 2016], and 2750 images from the Flick2K dataset [Lim *et al.*, 2017]. Before the training, all the color images are converted into gray-scale images. In each iteration during training, 64 patches of size 128×128 were randomly sampled from The SR we used to generate observations for training is set as 10%. The network parameters are optimized by minimizing the ℓ_1 loss with the ADAM [Kingma and Ba, 2014] optimizer. The learning rate (LR) starts from 10^{-4} and then decrease by half every 40000 iterations until 5×10^{-7}. the images and the patches are normalized to [0,1].

[1] https://www.cs.rochester.edu/~jliu/code/TensorCompletion.zip
[2] https://github.com/jamiezeminzhang/Tensor_Completion_and_Tensor_RPCA
[3] Implemented by ourselves based on the code of TNN
[4] https://github.com/TaiXiangJiang/Framelet-TNN
[5] https://taixiangjiang.github.io/
[6] https://github.com/seoungwugoh/opn-demo

Table 1: The quantitative results by different methods on the MRI data with different sample rates. The best and the second best values are respectively highlighted by red, blue.

SR	10%		20%		30%		Time
Method	PSNR	SSIM	PSNR	SSIM	PSNR	SSIM	(s)
Observed	8.09	0.043	8.60	0.070	9.18	0.099	—
HaLRTC	18.07	0.421	21.99	0.636	25.27	0.783	13.1
TNN	22.19	0.568	27.29	0.803	30.24	0.886	74.2
DCTNN	23.67	0.639	27.61	0.810	30.58	0.890	48.4
FTNN	25.05	0.755	29.05	0.884	32.06	0.936	362.3
DP3LRTC	28.38	0.878	32.56	0.948	35.44	0.972	201.4
OPN	16.08	0.376	19.03	0.515	24.54	0.781	17.2
CRUnet	27.63	0.876	31.87	0.946	35.77	0.976	6.3
DAP	28.24	0.884	32.57	0.951	36.39	0.978	121.1

3 MRI Data

We test our method and compared methods on the MRI[7] data of the size $142 \times 178 \times 121$. The random sampling rates (SRs) are selected as 10%, 20%, and 30%. Tab.1 exhibits the PSNR and SSIM values of results by different methods. Our method obtain the highest quality metrics except for the PSNR value when SR$= 10\%$. As the three modes of the MRI are all spatial direction, we illustrate the 110-th frontal slice, the 165-th horizontal slice, and the 50-th lateral slice of all results by different methods in Fig. 1. We can see that our method and CRUnet recover the frontal slice well while our method recoveries horizontal and lateral slices better.

[7] Available at https://brainweb.bic.mni.mcgill.ca/brainweb.

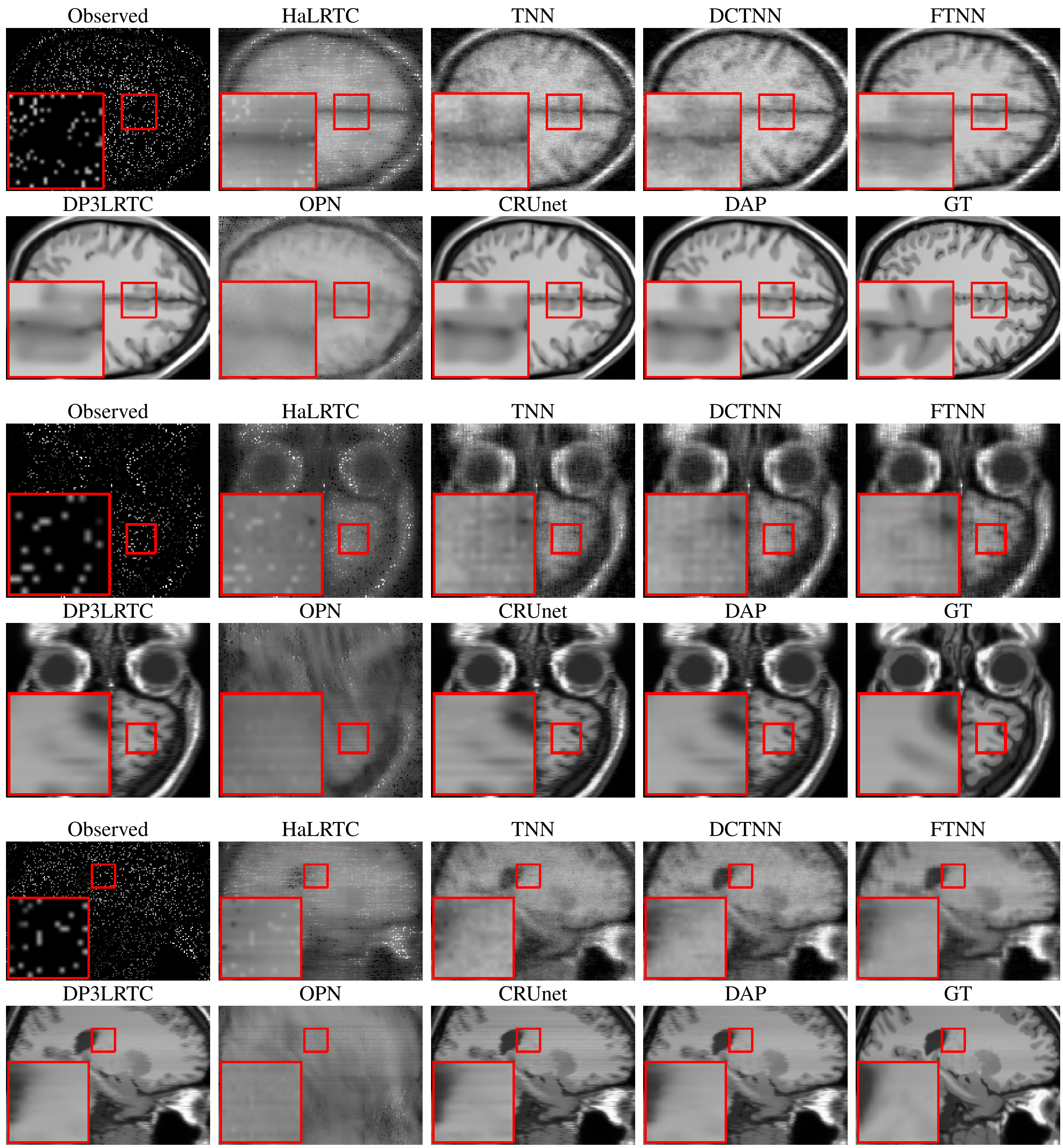

Figure 1: The 110-th frontal slice (top two rows), the 165-th horizontal slice (middle two rows), and the 50-th lateral slice (bottom two rows) of all results by different methods on the MRI data with SR = 10%.

4 Additional Results on Color Images and Videos

Tab.2 reports the PSNR and SSIM values of results on color images (*Airplane*, *House*, *Lena*, and *Redhosue*) by different methods with different structural missing types. The best and second best values are respectively highlighted in red and blue colors. Figs.2-5 shows the visual results by different methods on color images with different structural missing.

Tab.3 shows the PSNR values, SSIM values of the results on the video *Highway* with different numbers of miss-

Table 2: Quantitative metrics of the results by different methods on color images with different structural missing types.

Structural Missing	Type-4		Type-5		Type-6		Type-7		Time
Method	PSNR	SSIM	PSNR	SSIM	PSNR	SSIM	PSNR	SSIM	(s)
Observed	14.49	0.822	16.24	0.888	13.11	0.758	9.35	0.392	—
HaLRTC	31.21	0.958	33.59	0.968	26.51	0.919	24.20	0.789	27.1
TNN	27.19	0.919	27.05	0.943	20.14	0.845	22.65	0.760	6.4
DCTNN	31.65	0.967	34.12	0.974	26.18	0.916	24.35	0.799	3.4
FTNN	23.25	0.904	27.01	0.964	23.60	0.891	24.57	0.821	28.9
DP3LRTC	34.22	0.980	37.91	0.987	27.79	0.938	28.46	0.881	7.2
OPN	33.73	0.982	36.57	0.986	28.02	0.947	28.68	0.868	1.3
Deepfillv2	33.50	0.981	38.94	0.989	27.83	0.950	27.68	0.842	38.4
DAP	34.53	0.984	40.25	0.992	29.33	0.957	31.05	0.911	123.3

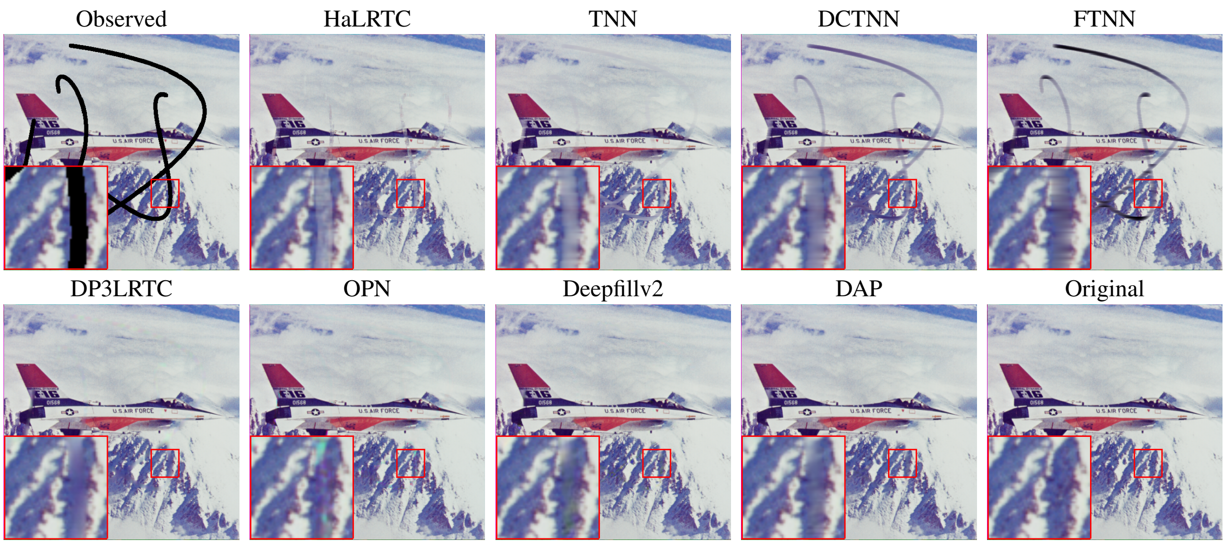

Figure 2: The visual results by different methods on the **color image** *Airplane*.

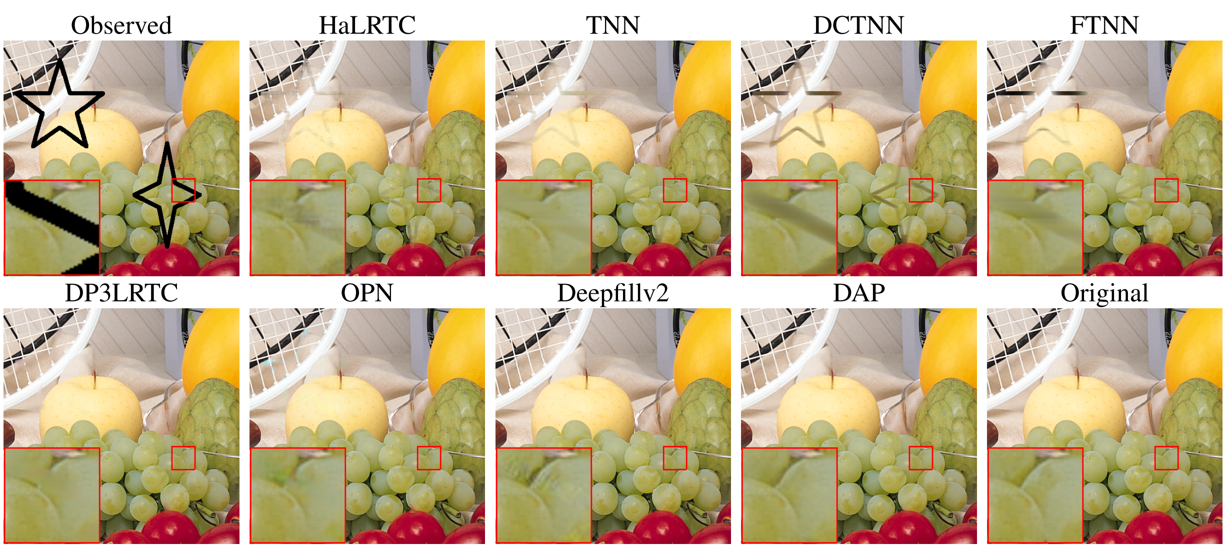

Figure 3: The visual results by different methods on the **color image** *Fruits*.

ing blocks (12 by 12). The visual examples of the results are shown in Fig.6. Tab.4 shows the PSNR values, SSIM values of the results on the video *Suzie* with different random sample rates. The visual examples of the results are shown in Fig.7.

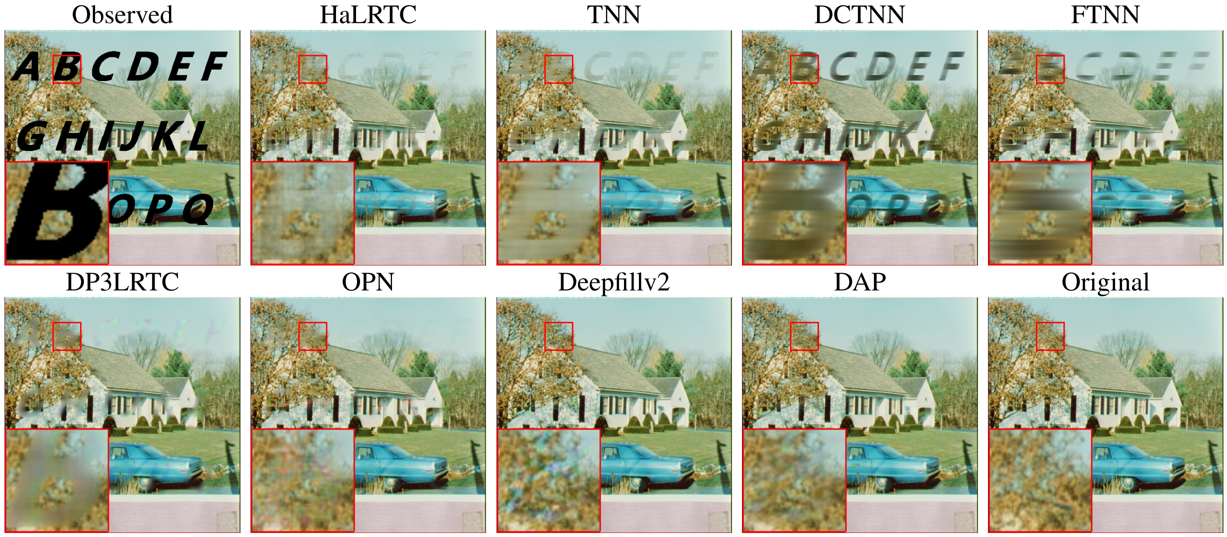

Figure 4: The visual results by different methods on the **color image** *House*.

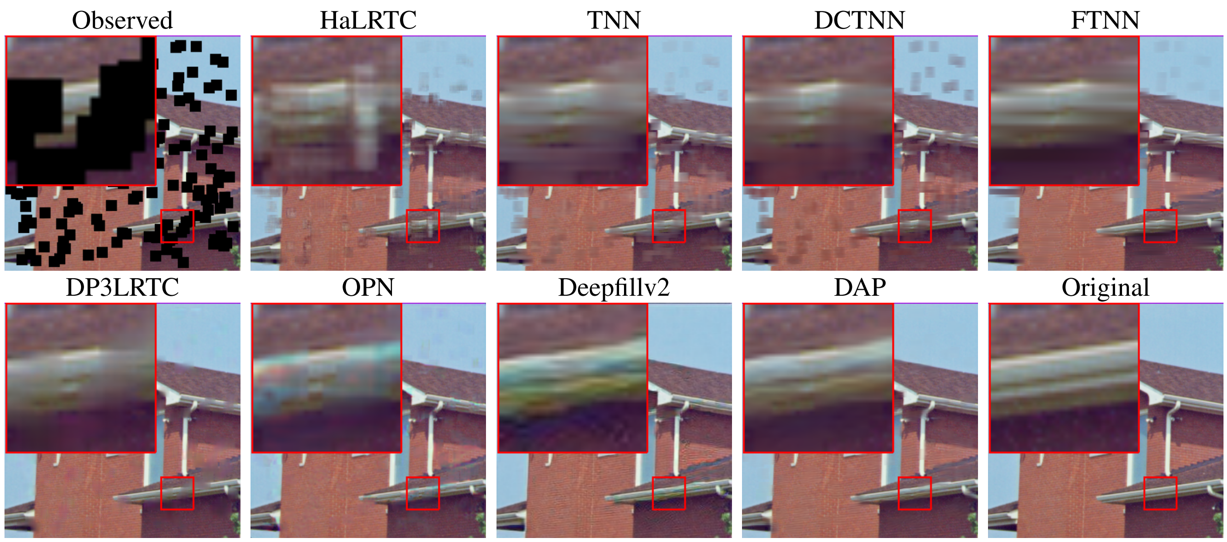

Figure 5: The visual results by different methods on the **color image** *Redhouse*.

Table 3: Quantitative results by different methods on the **video** *Highway* with different number of missing blocks (12 by 12).

Number	#50		#70		#90		Time
Method	PSNR	SSIM	PSNR	SSIM	PSNR	SSIM	(s)
Observed	9.25	0.517	7.56	0.326	6.70	0.272	—
HaLRTC	29.63	0.915	29.07	0.874	28.56	0.844	8.3
TNN	16.28	0.670	12.43	0.476	10.94	0.399	18.5
DCTNN	31.96	0.933	31.20	0.899	30.85	0.875	11.9
FTNN	31.34	0.932	29.40	0.881	27.57	0.863	263.6
DP3LRTC	32.85	0.944	32.14	0.918	32.71	0.907	46.7
OPN	34.95	0.952	32.64	0.924	32.90	0.914	12.0
Deepfillv2	33.64	0.940	32.61	0.917	32.57	0.906	3.7
DAP	35.03	0.953	33.44	0.930	33.39	0.920	98.2

Table 4: Quantitative results by different methods on the **video** *Suzie* for random missing.

SR	5%		10%		20%		Time
Method	PSNR	SSIM	PSNR	SSIM	PSNR	SSIM	(s)
Observed	6.61	0.009	6.84	0.013	7.36	0.019	—
HaLRTC	19.33	0.563	21.90	0.649	24.90	0.767	9.7
TNN	18.92	0.415	26.74	0.766	28.13	0.864	16.6
DCTNN	24.72	0.625	26.19	0.765	28.19	0.852	12.2
FTNN	25.21	0.745	27.62	0.826	29.00	0.897	106.1
DP3LRTC	26.19	0.810	28.01	0.870	29.47	0.922	46.5
OPN	19.77	0.605	19.76	0.629	24.11	0.759	5.2
CRUnet	26.17	0.813	28.02	0.877	29.50	0.928	1.0
DAP	26.37	0.817	28.20	0.881	29.58	0.932	17.1

Tab.5 shows the PSNR values, SSIM values of the results on the video *Bridge-far* with a random block missing. The visual examples of the results are shown in Fig.8. For all results, the temporal vectors in the missing area of the video *Bridge-far*,

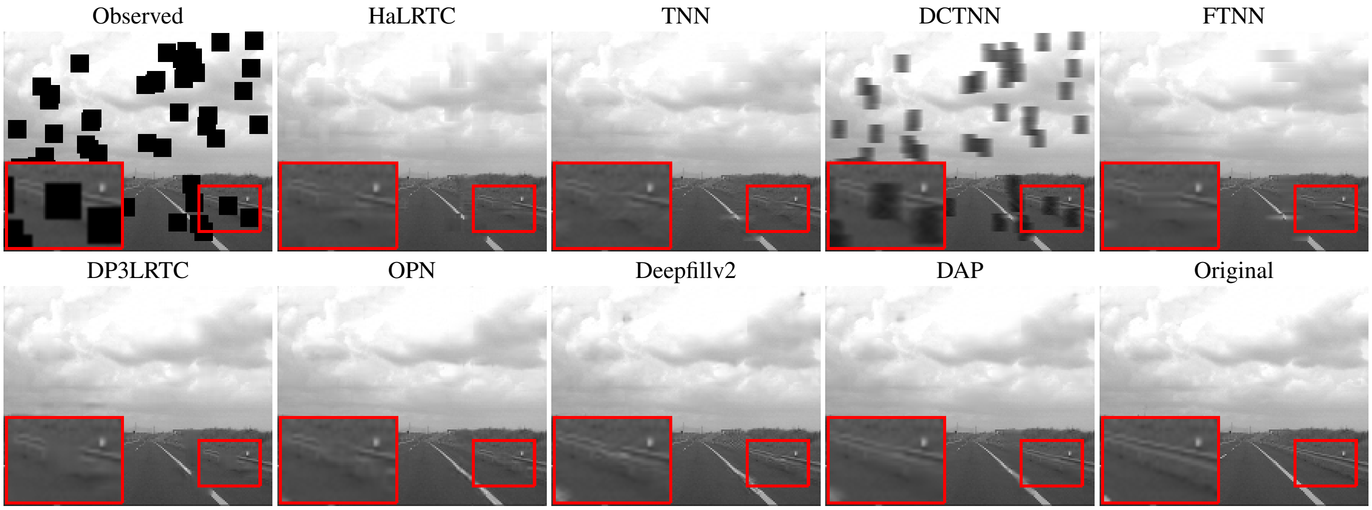

Figure 6: The visual results by different methods on the **video** *Highway* (the 39-th frame) with 50 blocks (12 by 12) missing.

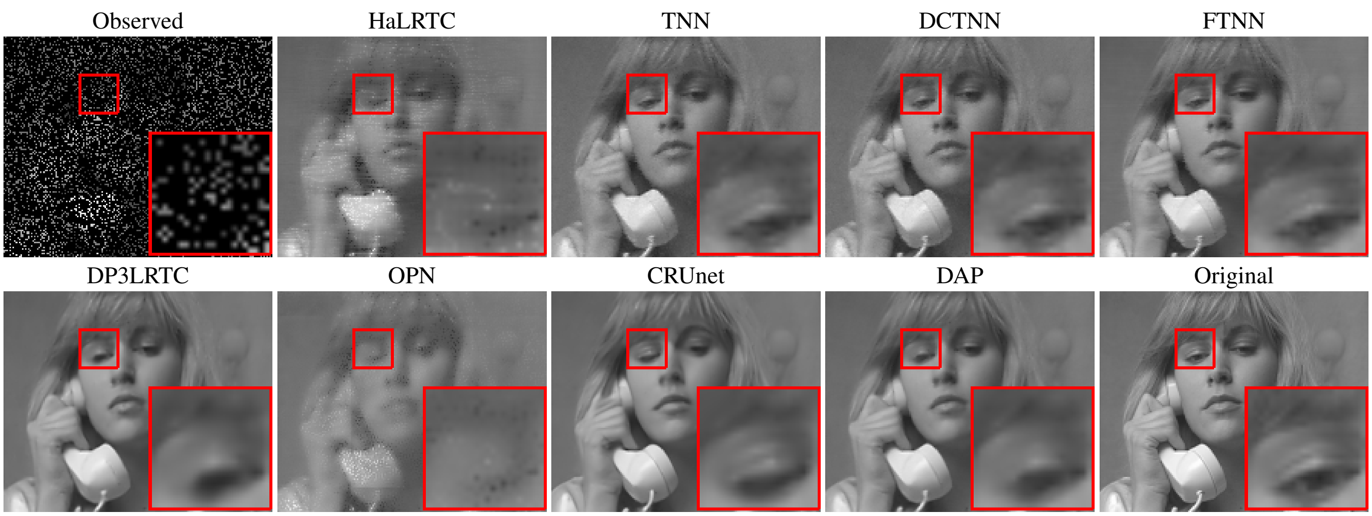

Figure 7: The visual results by different methods on the **video** *suzie* (the 1-st frame) for random missing with SR = 20%.

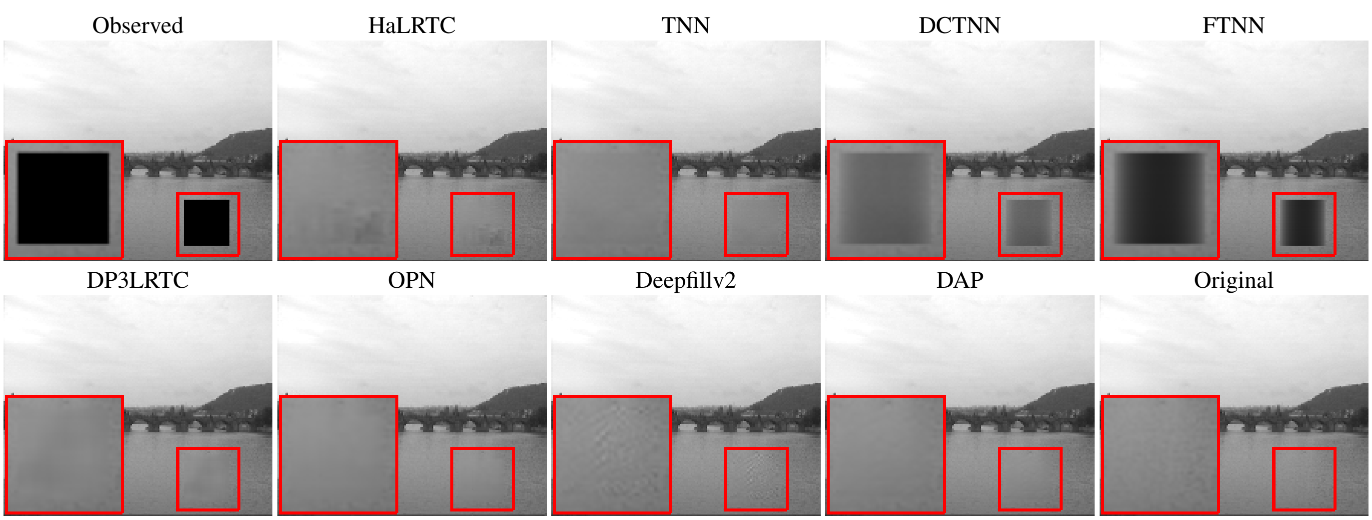

Figure 8: The visual results by different methods on the **video** *Bridge-far* (the 39-th frame) with a random block (30 by 30) missing.

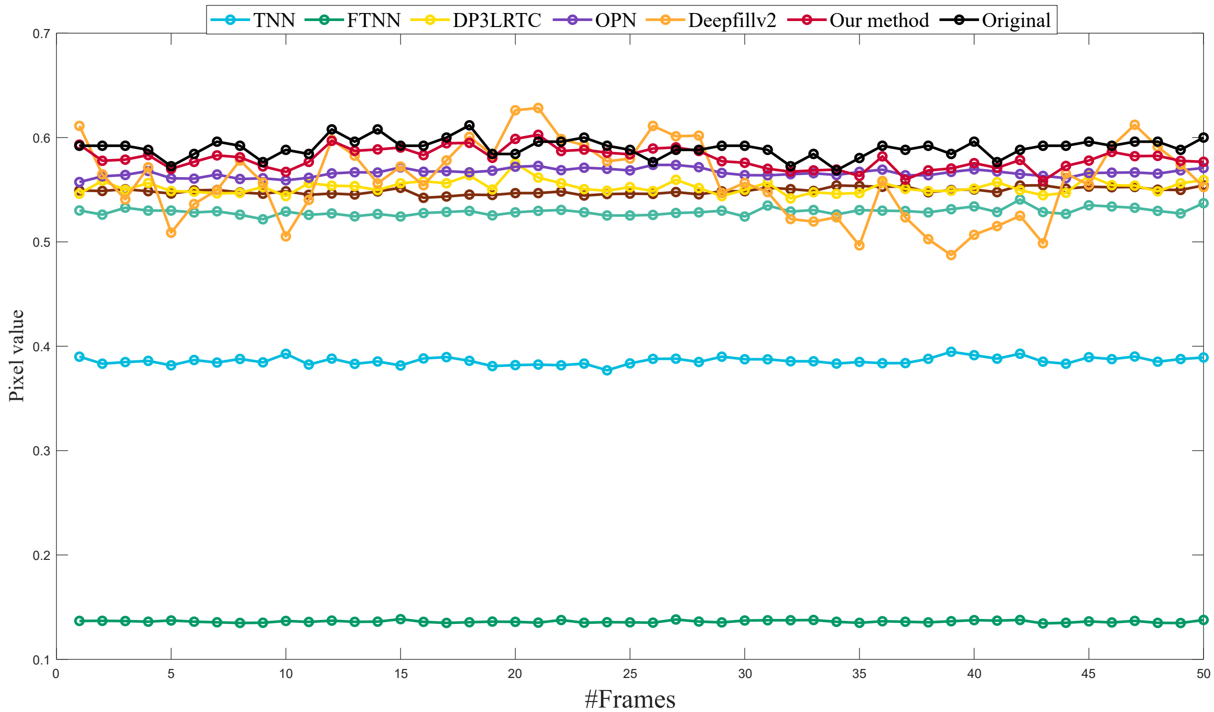

Figure 9: The temporal curves of the recovered **video** *Bridge-far* by different methods.

Table 5: Quantitative results by different methods on the **video** *Bridge-far* with a random block (30 by 30) misssing.

Video	*Bridge-far*		Time
Method	PSNR	SSIM	(s)
Observed	19.95	0.938	—
HaLRTC	47.87	0.993	3.6
TNN	31.45	0.975	19.6
DCTNN	47.65	0.994	24.5
FTNN	24.11	0.954	75.1
DP3LRTC	48.34	0.994	47.4
OPN	45.11	0.990	10.5
Deepfillv2	47.29	0.987	3.4
DAP	51.89	0.995	83.7

are plotted in Fig.9.

4.1 Additional Results on MSIs

In Tab.6, we list the quantitative metrics of the results by different methods on MSIs with different sampling rates. We display the pseudo-color images (composed by 25-th, 15-th, and 1-st bands) of the reconstructed MSIs by different methods in Fig.10.

References

[Chen and Pock, 2016] Yunjin Chen and Thomas Pock. Trainable nonlinear reaction diffusion: A flexible framework for fast and effective image restoration. *IEEE Transactions on Pattern Analysis and Machine Intelligence*, 39(6):1256–1272, 2016.

[Jiang *et al.*, 2020] Tai-Xiang Jiang, Michael K Ng, Xi-Le Zhao, and Ting-Zhu Huang. Framelet representation of tensor nuclear norm for third-order tensor completion. *IEEE Transactions on Image Processing*, 29:7233–7244, 2020.

[Kingma and Ba, 2014] Diederik P Kingma and Jimmy Ba. Adam: A method for stochastic optimization. *arXiv preprint arXiv:1412.6980*, 2014.

[Lim *et al.*, 2017] Bee Lim, Sanghyun Son, Heewon Kim, Seungjun Nah, and Kyoung Mu Lee. Enhanced deep residual networks for single image super-resolution. In *Proceedings of the IEEE conference on computer vision and pattern recognition workshops*, pages 136–144, 2017.

[Liu *et al.*, 2013] Ji Liu, Przemyslaw Musialski, Peter Wonka, and Jieping Ye. Tensor completion for estimating missing values in visual data. *IEEE Transactions on Pattern Analysis and Machine Intelligence*, 35(1):208–220, 2013.

[Lu *et al.*, 2019] Canyi Lu, Xi Peng, and Yunchao Wei. Low-rank tensor completion with a new tensor nuclear norm induced by invertible linear transforms. In *Proceedings of the IEEE Conference on Computer Vision and Pattern Recognition*, pages 5996–6004, 2019.

[Ma *et al.*, 2016] Kede Ma, Zhengfang Duanmu, Qingbo Wu, Zhou Wang, Hongwei Yong, Hongliang Li, and Lei Zhang. Waterloo exploration database: New challenges for image quality assessment models. *IEEE Transactions on Image Processing*, 26(2):1004–1016, 2016.

[Oh *et al.*, 2019] Seoung Wug Oh, Sungho Lee, Joon-Young Lee, and Seon Joo Kim. Onion-peel networks for deep

Table 6: Quantitative results by different methods on **MSIs** with random missing.

MSI	*Balloons*						*Clay*						*Paints*						
SR	3%			5%			3%			5%			3%			5%			
Method	PSNR	SSIM	SAM	PSNR	SSIM	SAM	PSNR	SSIM	SAM	PSNR	SSIM	SAM	PSNR	SSIM	SAM	PSNR	SSIM	SAM	Time (s)
Observed	13.41	0.114	—	13.50	0.136	—	15.83	0.391	—	15.92	0.408	—	10.45	0.084	—	10.54	0.103	—	—
HaLRTC	26.07	0.877	10.035	30.37	0.928	7.061	28.98	0.940	7.500	34.03	0.964	5.681	21.56	0.801	11.344	24.43	0.876	8.820	109.2
TNN	18.80	0.680	24.808	23.08	0.810	17.313	20.74	0.722	29.397	24.51	0.795	21.182	14.33	0.545	29.745	16.79	0.679	22.417	63.8
DCTNN	29.18	0.891	10.856	36.41	0.967	5.941	27.51	0.808	15.930	33.05	0.914	10.476	23.33	0.824	12.587	28.84	0.934	7.524	42.5
FTNN	38.02	0.986	3.391	41.05	0.993	2.622	35.10	0.971	4.552	37.67	0.985	3.885	28.82	0.952	6.106	31.98	0.979	4.260	667.9
DP3LRTC	38.28	0.978	4.682	40.92	0.990	3.141	38.81	0.929	7.645	41.68	0.979	5.018	28.61	0.941	6.120	31.99	0.974	3.879	731.8
OPN	11.97	0.402	29.121	16.09	0.500	25.452	9.16	0.169	55.584	15.39	0.259	47.390	10.35	0.223	31.912	13.36	0.295	29.426	4.8
CRUnet	38.38	0.989	3.124	40.95	0.994	2.115	37.04	0.980	5.867	41.58	0.990	3.853	28.21	0.954	4.892	31.74	0.979	3.476	4.3
DAP	39.52	0.991	2.725	42.11	0.995	2.067	39.98	0.987	4.485	42.67	0.992	3.762	28.96	0.959	4.523	32.18	0.980	3.308	166.4

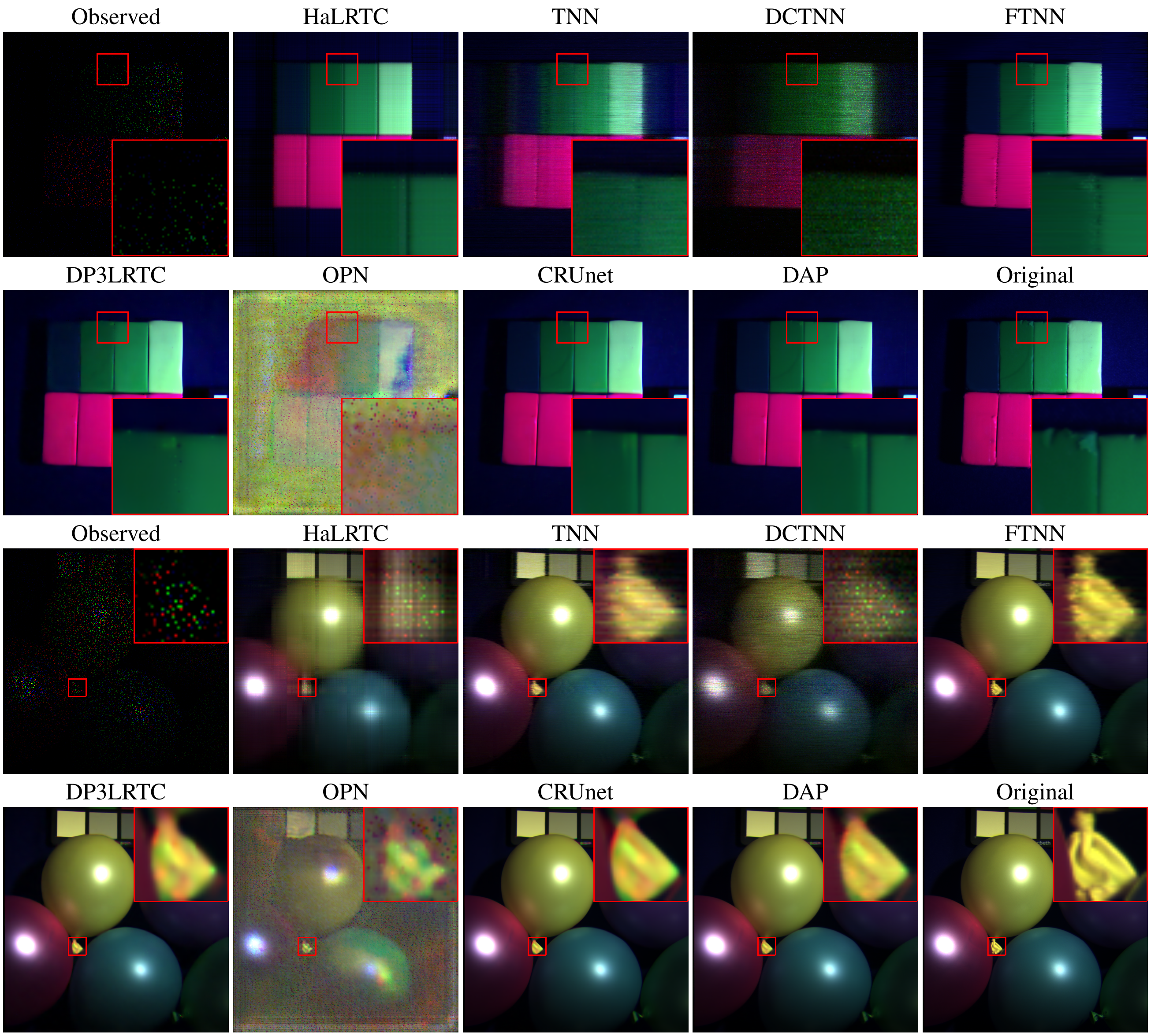

Figure 10: The pseudo color image (composed of the 25-th, 15-th, and the 1-st bands) of recovered results by different methods on **MSIs** *Clay* (top two rows) and *Balloons* (bottom two rows) with SR= 3% and 5%, respectively.

video completion. In *Proceedings of the IEEE/CVF International Conference on Computer Vision*, pages 4403–4412, 2019.

[Timofte *et al.*, 2017] Radu Timofte, Eirikur Agustsson, Luc Van Gool, Ming-Hsuan Yang, and Lei Zhang. Ntire 2017 challenge on single image super-resolution: Methods and results. In *Proceedings of the IEEE conference on computer vision and pattern recognition workshops*, pages 114–125, 2017.

[Wang *et al.*, 2004] Zhou Wang, Alan C Bovik, Hamid R Sheikh, and Eero P Simoncelli. Image quality assessment: from error visibility to structural similarity. *IEEE Transactions on Image Processing*, 13(4):600–612, 2004.

[Zhang and Aeron, 2017] Zemin Zhang and Shuchin Aeron. Exact tensor completion using t-SVD. *IEEE Transactions on Signal Processing*, 65(6):1511–1526, 2017.

[Zhao *et al.*, 2020] Xi-Le Zhao, Wen-Hao Xu, Tai-Xiang Jiang, Yao Wang, and Michael K Ng. Deep plug-and-play prior for low-rank tensor completion. *Neurocomputing*, 400:137–149, 2020.